Magnetoconductance in epitaxial bismuth quantum films: Beyond weak (anti)localization

Doaa Abdelbarey, Julian Koch,* Philipp Kröger, Priyanka Yogi, Christoph Tegenkamp,* and Herbert Pfnür†
Institut für Festkörperphysik, ATMOS, Leibniz Universität Hannover, Appelstraße 2, 30167 Hannover, Germany

(Received 12 May 2021; revised 9 July 2021; accepted 6 August 2021; published 17 August 2021)

The complex behavior of magnetoconductance of Bi films grown epitaxially on Si(111) with a thickness of 20–100 bilayers (BL) was measured at $T = 9$ K in magnetic fields up to $B = 4$ T, oriented in-plane parallel and perpendicular to the electric dc current I. Contributions to magnetoconductance (MC) by diffuse scattering, by weak localization (WL) as well as by weak antilocalization (WAL) were identified. All these components to MC turned out to be isotropic in two dimensions, i.e., no dependence on angle between B and I within the surface plane was found. Only for $B \perp I$ an *increase* of MC was detected that is, to first approximation, $\propto B^2$. It is ascribed to ballistic scattering between the Rashba-split interfaces that allow Umklapp scattering without spin flip. While MC within the surface states, dominant at small thicknesses, d, shows negligible diffuse scattering under the chosen geometry, their quantum corrections are characterized by WAL with $\alpha = -0.3$ and a coupling strength that decays $\propto 1/d$ with layer thickness. The admixing of quantized bulk states, which dominates MC above 50 BL, not only increases diffuse scattering, it introduces WL in combination with WAL. Presumably due to hybridization with the surface states, it also modifies strongly the WAL component for $d > 60$ BL. Thus our findings suggest an intriguing interplay in magnetotransport between 2D and quantized 3D states at the Fermi surface of ultrathin bismuth quantum films and provide further deep insight into the electronic transport in quantized and partly spin split bands.

DOI: 10.1103/PhysRevB.104.075431

I. INTRODUCTION

Bismuth is a semimetal that has attracted a lot of interest because of its unique electronic properties such as low carrier concentrations, high carrier mobilities [1,2] and a Fermi wavelength (λ_F) of ∼30 nm [3]. Because of these properties, several fascinating physical phenomena have been observed. Experimentally and theoretically, an intriguing entanglement between dimensionality and electronic properties has been reported. In quantized bismuth films, numerical calculations of the chemical potential and carrier density indicate that quantization plays a role when the film thickness is below 35 nm [4]. Furthermore, Park *et al.* [5] observed dimensional crossover for the quantum transport properties of Bi thin films when the film thickness exceeds the Fermi wavelength. Due to a negative indirect overlap in the Bi band structure [6], the electronic states are very susceptible to film thickness, position of Fermi level, and to spin-orbit coupling [7]. In addition to the unique band structure, Bi films have recently attracted further significant interest. Several groups have reported observations of linear magnetoresistance [8,9], which make Bi thin films attractive as magnetic-field sensors [10,11]. Several high-resolution angle-resolved photoemission spectroscopy experiments have been performed on Bi(111) films grown on Si(111) substrate and have revealed that there is an overlap of the surface state(s) with the bulk states near the $\overline{\Gamma}$ and $\overline{M}$ points of the Brillouin zone, so that surface resonance states (SRS) are formed [3,12–14]. Very recently, it was reported that the quantum well states at the $\overline{\Gamma}$ point behave like surface states [15]. On the other hand, the states close to the $\overline{M}$ point are spin degenerate [16] and the surface states in this k range lose their spin-split property, while the film preserves two-dimensional (2D) inversion symmetry [3]. This implies that the quantum well states are just quantized bulk states at the $\overline{M}$ point, and that surface and quantum well states are entangled [12,13,17,18]. Depending on the film thickness, the presence of SRS leads to coherent coupling between the surface and bulk conduction channels, which strongly affects the conductivity corrections [19,20].

Conduction is mainly limited by scattering processes at phonons and at defects such as impurities [21]. The magnetoconductance is a convenient tool to discriminate between different scattering mechanisms that have an influence on magnitude and sign of changes introduced by temperature and magnetic field [19,22]. In our recent work [23] on magnetotransport in ultrathin Bi films under perpendicular magnetic field we have found clear evidence for thickness dependent changes of magnetconductance (MC) induced by corresponding modifications of the band structure. Furthermore, there is a critical thickness around 60 BL (1 BL corresponds to a thickness, $d = 3.94$ Å) above which the quantum well states dominate the transport [23]. These results are consistent with the change in the dominant carrier sign at this critical thickness seen earlier [24]. For the B-field orientation normal to the surface, scattering processes within the surface or interface are strongly weighted in MC. In contrast, magnetotransport measurements with an in-plane B field put much more weight

*Now at Institut für Physik, Technische Universität Chemnitz, Reichenhainer Str. 70, D-09126 Chemnitz, Germany.
†Also at Laboratory of Nano and Quantum Engineering (LNQE), Leibniz Universität Hannover, Schneiderberg 39, D-30167 Hannover, Germany; herbert.pfnuer@fkp.uni-hannover.de

on scattering of charge carriers between the interfaces and on contributions from the quantum well states and their hybridization with the surface states [25–27]. Therefore, our study presented here with investigations of the same system under in-plane B fields parallel and normal to the current direction complements the previous study. Thus, we want to deepen the understanding of the MC of Bi films as a function of film thickness.

While much research in Bi films to date has concentrated on studies of MC under perpendicular fields using different techniques [19,23,28–33], very few measurements under parallel fields were reported in Bi thin films [32,33]. Indeed, to the best of our knowledge, there is no systematic study of the thickness dependence of MC with in-plane magnetic fields for Bi thin films on a Si(111) substrate, nor are there measurements at different angles between current and B field. In the study presented here we not only varied the thickness, d, between 20 and 100 BL in an in-plane field ($B_\parallel$) up to 4 T, we also measured with the in-plane B field parallel and perpendicular to the current direction. Furthermore, there was no need to cap the single crystalline Bi films by a protecting layer, since our measurements were carried out *in situ* so that we kept a bare interface on the vacuum side. This fact allows us to exploit symmetry properties between the interfaces: Growth of Bi films on Si(111) substrates by molecular beam epitaxy not only generates closed films while the interaction with Si is still sufficiently weak in order not to modify the interface properties strongly in comparison with the vacuum interface. Thus we not only deepen further our insight into the conductive properties of these films, but also obtain some unexpected results not seen on films with reactive capping layers [32,33].

Here we present results with the B-field orientation in-plane, both parallel and perpendicular to the current direction. Under these conditions, we show that, depending on thickness, d, changes of band structure and of their quantization, together with the entanglement of surfaces and bulk-derived quantum well states, lead to characteristic signatures in magnetoconductance and in quantum corrections. This complex interaction leads to four different mechanisms in magnetotransport. These turn out to be only in part isotropic (i.e., indendent of B-field direction relative to electric current direction). In-plane (2D) isotropy was found for diffuse scattering, which is anisotropic in the third dimension. Furthermore, quantum corrections described by weak antilocalization (WAL) for the surface states, and by weak localization (WL) for quantum well states turn out to be also 2D isotropic. Surprisingly, a strongly 2D-anisotropic fourth component was found, which increases MC as a function of B and exists only for B normal to the current. It will be discussed within a tentative model at the end of the paper.

II. EXPERIMENTAL DETAILS

All experiments were performed under ultrahigh vacuum conditions at a base pressure of 7×10^{-11} mbar. Low-doped Si(111) samples ($\rho > 1000\,\Omega$cm) of size $15\times15\times0.5\,\text{mm}^3$ were used for the conductivity measurements. Four slits were machined into the samples in order to prevent crosstalk between the eight electrical $TiSi_2$ contacts for transport measurements (Fig. 1). Details about the fabrication of contacts

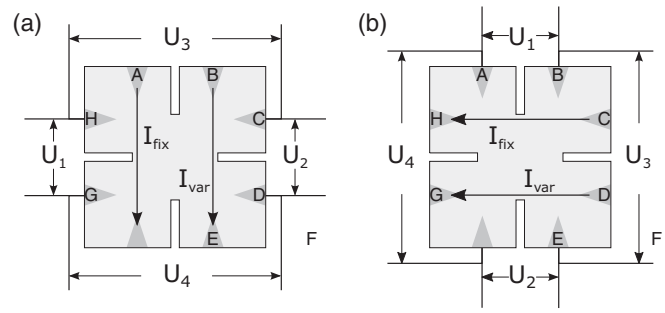

FIG. 1. Schematic (top view) of the setup for current and voltage measurements with 8 contacts (A to H). For details, see text.

as well as about the *in situ* cleaning procedures are described elsewhere [28]. Bi was evaporated out of a ceramic crucible heated by a W filament. The amounts were controlled by a quartz microbalance. Pure films were grown at 200 K followed by annealing to 410 K for several minutes. The layer thickness of the Bi films is given in bilayers (thickness of 1 BL, $d = 3.94$ Å, as already mentioned).

The Bi coverage was calibrated with the help of the $\sqrt{3}\times\sqrt{3}$ reconstructions on Si(111) and by recording bilayer oscillations in conductance during evaporation. The deposition rate was 1 BL per minute. The morphologies of the Si-substrates and the epitaxial films were checked by low energy electron diffraction.

The transport setup allows us to measure DC conductance G as a function of temperature down to 9 K. In order to ensure that the current has no components perpendicular to the desired direction of measurement, we use a symmetrized eight-point measurement as shown in Fig. 1, which is a combination of two four-point measurements. A fixed current I_{fix} is applied as well as a variable current I_{var}, which is adjusted at the beginning of the measurement (at zero magnetic field), so that the voltages U_3 and U_4 are minimal, and then kept constant throughout the measurement. The conductance is determined via $G = (I_{\text{fix}} + I_{\text{var}})/[1/2(U_1 + U_2)]$. We further refer the interested reader to Refs. [28,34] and [23] for more details.

Most important in the present context, our setup allows a rotation of the sample so that the magnetic field can be oriented normal and parallel to the surface plane (or any angle in between). The various contacts allow to have the in-plane B-field either parallel ($B_\parallel \parallel I$) or perpendicular ($B_\parallel \perp I$) to the current direction by mounting the sample such that B is aligned parallel to the sample surface and to one of the sample edges. Switching the current direction between the configurations (a) and (b) of Fig. 1 allows the current to flow either parallel or perpendicular to the B field. A magnetic field up to ±4 T is applied using a superconducting split coil magnet. Due to the location of the contacts at the edges of the sample in this setup, the relation between conductivity, σ, and the measured conductance, G, is close to 1. Therefore, we set $\sigma = G$.

III. RESULTS

We divide our results into those that are independent of relative orientations between electric current I and magnetic field $B_\parallel$ within the surface plane, which we call 2D isotropic,

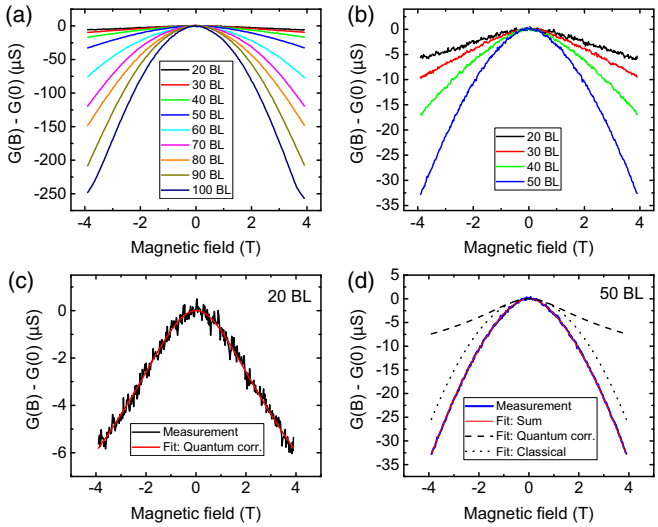

FIG. 2. Magnetoconductance with in-plane orientation of the B field parallel to the current direction ($B_\parallel \parallel I$) as a function of film thickness, measured at 9 K. (a) Compilation of data for all thicknesses. (b) Magnification for d between 20 and 50 BL. (c) 20 BL curve with fit (red line) assuming only WAL (for details, see text). (d) Fit for $d = 50$ BL including also a classical contribution.

and those that are not. The test of 2D isotropy was done by subtracting the MC curves $G(B_\parallel \perp I)$-$G(B_\parallel \parallel I)$, which results in complete disappearance of the 2D-isotropic contributions. These will be discussed first. The contribution to MC with an explicit dependence on the relative angle between I and B is described in Sec. III B.

A. 2D-isotropic parts of magnetoconductance with B in plane

As a starting point, we present the results of magnetoconductance with the DC current and B field parallel to each other ($B_\parallel \parallel I$) as a function of layer thickness d. These data were obtained on the same series of bismuth samples as in Ref. [23], in which the magnetoconductance in a perpendicular magnetic field was studied. The B field induced changes of conductance at 9 K, $\Delta G = G(B) - G(0)$, (MC), are plotted in Fig. 2(a) as a function of film thickness ranging from 20 to 100 BL for the in-plane orientation of the B field.

We observe a negative MC for all thicknesses. Starting from values below 10 μS at 20 and 30 BL, we note not only an increase of magnitude, particularly above 50 BL, but also a gradual change of the curve shape from an almost linear shape above 1T at 20 BL to a more parabolic shape at higher d.

In analogy to the analysis in magnetic fields perpendicular to the surface [23], we assume for layer thicknesses up to 50 BL that essentially two mechanisms contribute to MC: Classical diffuse scattering due to the Lorentz force acting now perpendicular to the surface plane, and a quantum correction, which adds a positive contribution at zero field, i.e., it corresponds to WAL.

WAL originates from spin dependent scattering, which according to a detailed theoretical analysis [15] happens mainly within the Rashba-split surface states. Therefore, we use a model of two closely spaced coupled 2D layers as a representation of the surface states for this contribution to the MC, containing a 2D (isotropic) electron gas with scattering defects, which has been investigated by several authors [35–38]. For an in-plane magnetic field B, ΔG within this model takes the form [25]:

$$\Delta G(B) = \alpha \frac{e^2}{2\pi^2\hbar} \ln\left(1 + \beta \frac{e^2 d^2 l_\Phi^2}{\hbar^2} B^2\right), \tag{1}$$

d is the distance between the interfaces and l_Φ is the phase coherence length. β describes the coupling strength between the layers ($0 < \beta \leqslant 1$, $\beta = 1$ for strong coupling). For an ideal 2D Fermi gas α is predicted to take the value of -0.5 per conducting channel in case of dominant spin-dependent scattering. This model turns out to be sufficient for the description of the quantum correction up to a layer thickness of 50 BL.

For an in-plane magnetic field the Lorentz force acts perpendicular to a 2D electron gas, i.e., the contribution of the surface states to the classical part of the magnetoconductance is expected to be negligible in this case. Therefore contributions to the classical part of MC should stem only from the bulk-derived quantum well states. This assumption is justified by our observations described below. Moreover, the only quantum well state that can make a significant contribution to the conductance is the one that crosses the Fermi level near the $\overline{M}$ point [15]. The states that cross E_F close to the $\overline{\Gamma}$ point [15] have a low density of states, and will be neglected as a first approximation. Based on these assumptions, we use a single-band model [39] to describe the classical contribution to the magnetoconductance:

$$G_{qw}(B) = G_{qw}(0) \frac{1}{1 + (\mu_{n,qw} B)^2}. \tag{2}$$

Here G_{qw} is the contribution of the quantum well state near the $\overline{M}$ point to the conductance and $\mu_{n,q}$ is the mobility of the electrons in this state. This model is indeed compatible with the data, as we will show below.

1. Classical contribution to MC

Using the two models just described, we now analyze the MC data with $B_\parallel \parallel I$ shown in Fig. 2 by fitting the MC data with Eqs. (1) and (2) and show that these two models are sufficient to perfectly describe the data up to $d = 50$ BL. At larger d, a WL contribution from quantum well states has to be taken into account (see Sec. III A 3).

While the behavior for the thinnest 20 BL film is fully described by Eq. (1) without classical part [see Fig. 2(c)], the sum of Eqs. (1) and (2) is required to describe the measured MC curves in Fig. 2 for higher film thicknesses, as shown exemplarily for $d = 50$ BL in Fig. 2(d).

Amplitude of MC. The amplitude of the classical part is shown in Fig. 3(a) as the difference $G_{qw}(0) - G_{qw}(4T)$. A strong increase of this amplitude is observed for $d > 40$ BL. This increase can clearly be correlated with the occupation of the quantum well state close to the $\overline{M}$ point of the Brillouin zone that is gradually lowered in energy as a function of d [12,15] starting around 30 BL [17]. This state contributes significantly to conductance due to its high density of states.

From this observation we conclude that the conductance within the surface states yields a negligible classical component to the MC [33,40]. This result is remarkable in the

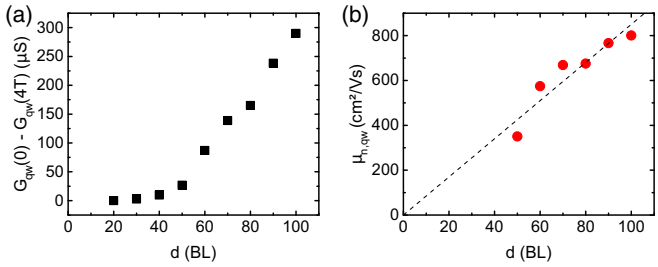

FIG. 3. Classical magnetoconductance: (a) Amplitude of diffuse scattering, quantified as $G_{qw}(0) - G_{qw}(4T)$, as a function of d. (b) Mobilities as obtained from the one-band model fit of magnetoconductance [Eq. (2)] with the B field parallel to the surface as a function of d. The dashed line represents a linear fit of the data that is compatible with an extrapolation to zero.

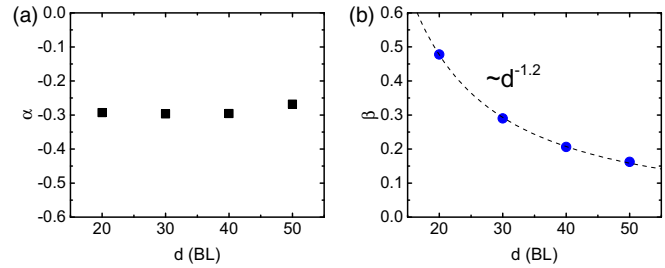

FIG. 4. WAL contribution, as expressed by the amplitude α (a) and coupling strength β (b) within the model of Ref. [25] and derived from the fits of MC according to Eq. (1), presented in Fig. 2.

sense that the wave functions of coupled surface states have a finite amplitude throughout the whole thickness and thus have a finite extension normal to the interfaces. The resulting conduction in this direction, however, seems to be sufficiently low so that the MC was not measurable under these conditions.

This observation also validates the model for the classical contribution in Eq. (2). Since the derived mobilities depend on $G_{qw}(0)$, which is only part of the total conductance, we estimated $G_{qw}(0)$ by assuming a thickness independent contribution of the surface states to the overall conductance at zero magnetic field $G_{ss}(0)$ determined from the extrapolation of $G(0, d)$ to $d = 10$ BL ($G(0) = G_{ss}(0) + G_{qw}(0)$).

Mobilities. The mobilities for the electrons in the quantum well state near the $\overline{M}$ point are shown in Fig. 3(b). Due to the high uncertainty at 30 and 40 BL, arising from the low value of $G_q(0)$ there, no values were evaluated. From the linear increase of the mobilities as a function of d, measured under the condition of a parallel B field, we conclude that interface scattering is the dominant mechanism that limits the mobilities. A similar conclusion was drawn from measurement with B normal to the surface [23]. Since with B oriented normal to the surface, as in Ref. [23], both surface and quantum well states contribute to MC, averaged values of mobilities were obtained there. Therefore, no anisotropy of mobilities has to be assumed to explain the larger mobilities of Fig. 3(b) compared to those of Ref. [23].

2. Weak Antilocalization

Determination of α. The fitting results for the quantum correction for $d = 20 - 50$ BL are shown in Fig. 4. For the fits we took the same $l_\Phi = 62$ nm value that was found with $B_\perp$ [23], which is valid as long as the scattering processes happen predominantly within the surfaces. In this thickness range the quantum correction can be described by Eq. (1). For higher thicknesses the equation has to be modified, which will be discussed in the next section.

As seen from Fig. 4(a) α stays constant at a value of $\alpha = -0.29 \pm 0.03$ in this thickness range. This value of α is significantly smaller than the value of -0.5 expected for 2D thin films or coupled sheets of free 2D electron gases characterized by a single transport channel [25,35–38]. This finding may not be all too surprising, since the band structure strongly deviates from that of a free electron gas [16,17] and exhibits multiple crossings of the Fermi level within the Brillouin zone, so that the value of α can only be taken as an effective, averaged, value.

In contrast to the constant values of α in Fig. 4(a), α decreases with film thickness d in a magnetic field $B_\perp$ perpendicular to the substrate surface [23], which we attributed to the interaction between the two interfaces and their decoupling with increasing d [23]. However, unlike the model used in the $B_\perp$ case, which assumes only a single transport channel within the 2D electron gas, the model in Eq. (1) considers two interacting 2D electron gases and describes the coupling strength via the parameter β, so that α is independent of the interface coupling.

Coupling between interfaces. As shown in Fig. 4(b), the coupling parameter β decreases $\propto (1/d)^{1.2}$ from 0.48 ± 0.04 at 20 BL to 0.16 ± 0.03 at 50 BL. This strongly deviates from an exponential dependence expected in the case of coupling exclusively due to quantum tunneling, indicating a finite conductance of the bulk due to the quantum well states and a coupling of the surface states to those states. Interestingly, the decrease of β with increasing d is overcompensated by the factor d^2, so that the argument of the logarithm in Eq. (1) actually increases with increasing d.

3. Combination of WAL and WL for $d > 50$ BL

The dominance of the contribution of the quantum well state to MC with itse high density of states for $d > 50$ BL, turns out to modify not only the observable quantum corrections. This fact becomes most visible from an analysis of the data measured with the B field still in plane, but perpendicular to the current direction ($B_\parallel \perp I$, see Fig. 5).

In fact, as we will show by the detailed analysis below, the MC data for $d > 50$ BL are governed by three main parts:

(a) The diffuse classical background that has already been discussed.

(b) Quantum corrections that have already been seen with $B_\parallel \parallel I$ and d up to 50 BL. Above 50 BL their behavior is strongly modified and a component of WL appears in addition, associated with the quantum well states. Also this contribution turns out to be 2D isotropic, but it is more difficult to be recognized in the configuration $B_\parallel \parallel I$.

(c) When we subtract $G(B_\parallel \perp I) - G(B_\parallel \parallel I)$, both the contributions of the classical scattering and the quantum corrections disappear, giving clear evidence that they are 2D

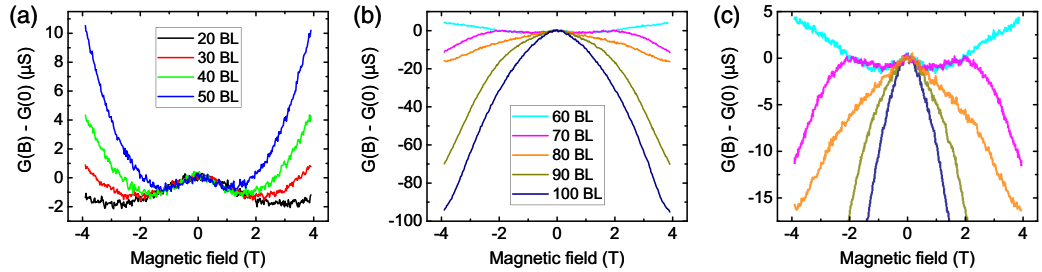

FIG. 5. B-field dependent contributions of conductance with in-plane orientation of the B field perpendicular to the current direction ($B_\parallel \perp I$) as a function of film thickness, measured at 9 K. (a) $d = 20-50$ BL. (b) same but for $d = 60-100$ BL. (c) magnification of (b).

isotropic. The remaining contribution to the MC is positive and depends quadratically on B. As will be discussed in detail in Sec. III B, this part does not originate from WL.

As a continuation of the previous section, we now discuss the 2D-isotropic quantum corrections for $d > 50$ BL. The changes compared to smaller thicknesses become best visible in the MC curves at small B fields [see Figs. 5(a) and 5(c)]. Comparing Figs. 5(a) and 5(c), the dip in the center around $B = 0$ sharpens up considerably. This indicates a drastic change in the scattering process that leads to the quantum correction. In order to fit the sharp central peak, β and/or l_Φ have to be increased drastically when going from 50 to 60 BL. However, this assumption alone does not yield a consistent description of the data. In particular, the winglike features of the 60 and 70 BL curves in Fig. 5(c) cannot be fit correctly. Therefore, staying within the WL-WAL-picture, a WL-like contribution in addition to the WAL contribution is required to describe the measured MC curves for $d \geqslant 60$ BL. Extending the discussion from above, this behavior must be the consequence of the admixing of a conductance contribution from the quantum well state, which becomes important above 50 BL. This state shows little spin polarization [15], but hybridizes with the surface states to form a surface resonance [3,12,14,16]. Therefore, this admixing must be responsible both for the WL-like contribution and for the modification of the WAL quantum correction.

There are two possibilities for the origin of this WL-like contribution. The first possibility becomes evident when considering quantum correction of the whole film in a more universal form [27,35,37,41]:

$$\Delta G(B) = N\frac{e^2}{2\pi^2\hbar}\left[\frac{3}{2}\ln\left(1+\frac{B^2}{B_1^2}\right)-\frac{1}{2}\ln\left(1+\frac{B^2}{B_\Phi^2}\right)\right], \quad (3)$$

where N is the number of conducting channels. The scaling fields $B_1 = \sqrt{\frac{\hbar^2}{\beta e^2 d^2 l_1^2}}$ and $B_\Phi = \sqrt{\frac{\hbar^2}{\beta e^2 d^2 l_\Phi^2}}$ contain β as well as the scattering lengths l_1 and l_Φ. $l_1 = (l_\Phi^{-2} + 2l_{so}^{-2})^{-1/2}$ is a combination of l_Φ and the spin-orbit scattering length l_{so}. In the extreme cases $l_{so} \ll l_\Phi$ (WAL) and $l_{so} \gg l_\Phi$ (WL) Eq. (1) is obtained with $N = 0.5 \cdot \alpha$ or $N = \alpha$, respectively.

Indeed, by means of Eq. (3) the MC data for $d \geqslant 60$ BL can be described accurately. The fitting results in the form of the scaling fields B_1 and B_Φ are plotted in Fig. 6(a) as a function of layer thickness. We only give the scaling fields since a separate determination of β and the scattering lengths is not meaningful with the available data. For $d = 60-80$ BL an optimal value of $N = 0.6$ is obtained, which corresponds to $\alpha \approx -0.3$ used for lower thicknesses. At 90 and 100 BL the classical background becomes so large that N cannot be determined unambiguously. Here we kept the same value as for the lower thicknesses. In addition, for $d \leqslant 50$ BL B_Φ was determined from the data in Fig. 4.

From 20 to 50 BL B_Φ slowly decreases as a function of d [Fig. 6(a)], since the product βd^2 is increasing with increasing d, as discussed in the previous section. This WAL contribution, however, is strongly modified when the new conduction channel due to the quantum well state becomes dominant, as seen by the change in B_Φ by almost a factor of 2 when d exceeds 50 BL.

Moreover, the field B_1 becomes non-negligible due to the strong increase of the spin orbit scattering length, which is now, according to our fits, in the same order of magnitude as the phase coherence length l_Φ. As a result, the condition $l_{so} \ll l_\Phi$, which is the prerequisite for a purely WAL-based quantum correction, does not hold true anymore, so that the more universal form of the quantum correction in Eq. (3) has to be used. The reduction of the spin orbit scattering can be explained by the admixture of the essentially unpolarized quantum well state(s), compared with the situation below 50 BL (see also Ref. [23]).

The field B_1 is associated with a positive term that dominates at larger B and leads to a w-shaped quantum correction, as shown in Fig. 6(b) for $B_\parallel \parallel I$. In this configuration the quantum correction is almost negligible compared to the large classical background.

Indeed, we were only able to determine its shape due to the measurements with $B_\parallel \perp I$, where the classical background and the parabolic quadratic term, which will be discussed

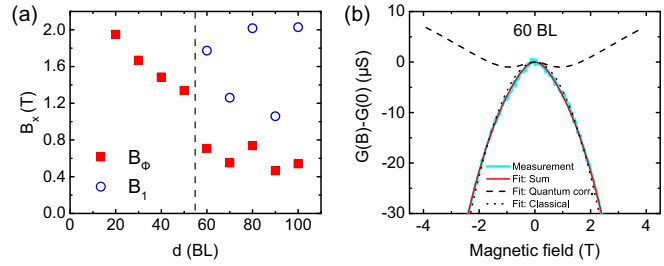

FIG. 6. Quantum correction: (a) Effective scaling fields B_1 and B_Φ as a function of layer thickness d, appearing in the terms of Eq. (3). (b) Visualization of the quantum correction contribution to the MC for $d = 60$ BL and $B_\parallel \parallel I$.

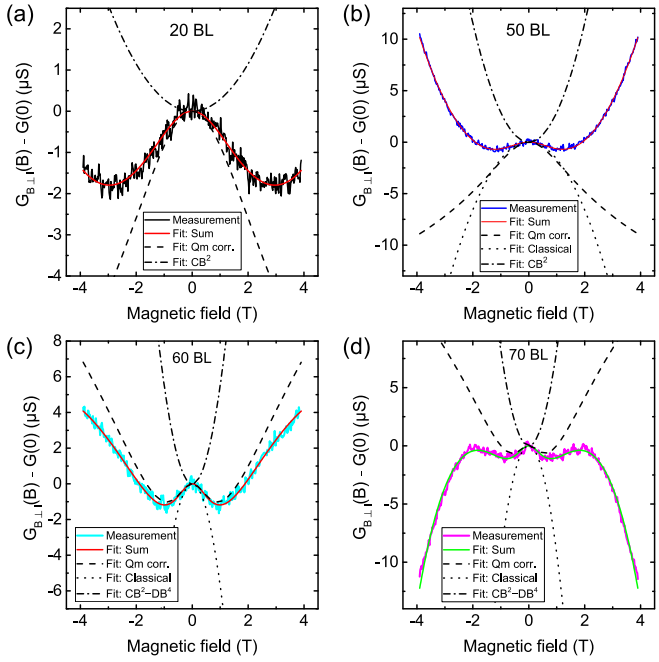

FIG. 7. Visualization of the various contributions to the magnetoconductance, as obtained by fits at 20 (a), 50 (b), 60 (c) and 70 BL, respectively. Long dashes: WAL and WL; dots: diffuse background; dashed-dotted: anisotropic contribution.

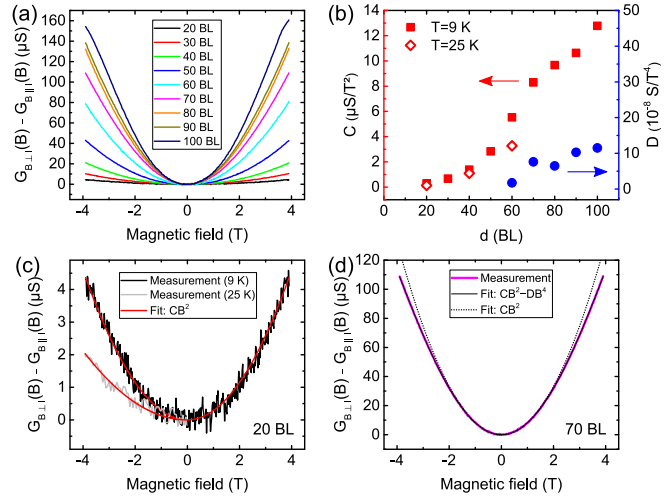

FIG. 8. (a) Residual magnetoconductance $\Delta G(B \perp I) - \Delta G(B \parallel I)$ at fixed d for d between 20 and 100 BL at $T = 9$ K. (b) Prefactors C, D of the quadratic and fourth-order terms, respectively [see inset (d)], of the fitting curves of (a) (closed symbols) as well as curves recorded at $T = 25$ K (open symbols). (c) 20 BL (at 9 and at 25 K) and (d) 70 BL (9 K) curves together with fits.

in the next section, partially cancel each other. The separation into the various contributions is shown in Fig. 7. This cancellation is particularly pronounced at 60, as shown in Fig. 7(c) so that the curve shape is dominated by the quantum correction.

While B_1 and B_Φ seem to be directly coupled, the large variation of values at different d between 60 and 100 BL reflects small differences in preparation of these layers that was also seen, but with a much smaller amplitude, in DC conductance. Therefore, the values of the scaling fields seem to be essentially independent of layer thickness for $d \geqslant 60$ BL.

The second explanation for the WL-like contribution is an actual WL contribution that comes directly from the quantum well states, instead of indirectly through the modification of the spin orbit scattering length of the surface states. However, in both cases the admixture of the quantum well states is responsible for the appearance of a positive quantum correction and for an abrupt increase of either β or l_Φ of the surface states is required to explain the sharpening of the central peak from 50 to 60 BL.

Again the hybridization of surface and quantum well states seems to be responsible for this finding, which allows dynamic charge transfer between the surface and quantized bulk states [42]. Thus for $d \geqslant 60$ scattering paths involving the whole volume become important, while at smaller d the conducting electron density is confined mainly within the surface states. Secondly, the mobilities that increase with d are coupled with the scattering times, and make scattering between both interfaces more likely. Turning this argument around, it seems that the quantum well states act as an efficient transmitter of electrons being scattered at the surfaces of the film without altering the spin.

On the other hand, the consistent description of combined WAL and WL with a single channel corroborates our assumption made above that the electron density in quantum well states seen close to Γ [15] that should lead to a sum of contributions of individual channels [43], is in fact negligible in our context.

Since both WAL and WL contributions turned out to be 2D isotropic, it seems that hybridization of top and bottom interfaces and to their hybridization with the quantized bulk states that are clearly effective here, are not the origin of any anisotropy [44]. Similarly, the combination of both Rashba [45] and Dresselhaus [46] spin-orbit coupling that must be present in this system, do not lead to predicted anisotropies [47–49] in the system investigated here.

B. Anisotropic contributions to magnetoconductance

As already mentioned above, the subtraction of the MC curves measured with $B_\parallel \parallel I$ from the curves of Fig. 5 results in a positive residual magnetoconductance that is shown in Fig. 8. This procedure is possible here, because both measurements were carried out on the same layers by just turning the current direction with respect to B using a second set of contacts. We also want to mention that this result is not dependent on sample orientation, but only on the angle between B and I: the same result was obtained by turning the sample by 90° around the surface normal.

The curves obtained from the difference between MC in both B-field directions are, to a very good approximation, simple parabolas, as shown by the exemplarily fitted curves [Figs. 8(c) and 8(d)] and by the relative amplitudes, C and D, of quadratic and higher order terms, respectively [Fig. 8(b)]. Only at $d \geqslant 70$ BL are there small higher-order corrections.

It is interesting to note that the thickness dependence of the amplitude of this anisotropic residual MC follows closely the

magnitude of the diffuse component of MC [see Fig. 3(b)]. This strongly suggests that both phenomena are associated with the increasing contribution of quantum well states to conductance, as already described above.

Since we have already discussed their WL properties that turned out to be 2D isotropic, there should not be a further anisotropic contribution from WL. In fact, neither the dependence on d nor the B dependence are compatible with WL: The increasing amplitude C [see Fig. 8(b)] that raises approximately linearly as a function of d above $d = 50$ BL would imply a correspondingly increasing number of conducting channels. Indeed, theoretical calculations show that the number of subbands crossing E_F close to $\overline{\Gamma}$ increases with d [50], but due to a very low density-of-states their contribution to conductance is negligibly small, as evident from the constant concentration of charge carriers for $d \geqslant 60$ BL [23]. Therefore, these states cannnot account for the observed increase of MC nor for this anisotropic contribution.

Also the magnetic field dependence, which should then be describable within the formalism of Eqs. (1) or (3) does not yield a behavior $\propto B^2$, or it requires the insertion of parameters that do not seem to be physical.

Finally, the observed small dependence on temperature also makes a significant contribution of WL quite unlikely. In data, taken at 25 K on different samples, which show almost the same overall conductance as those mostly investigated here, the amplitude C compared to that at 9 K changes only by a factor of 2. In contrast, WL should be sensitive to a reduction of the phase coherence length and thus be much more strongly reduced. We note that this positive contribution to MC turned out to be still visible even at a temperature of 100 K. At this temperature the amplitude is indeed damped and the dependence on B is close to linear. However, no systematic investigations were carried out at elevated temperatures.

For these reasons, we suggest an alternative mechanism for this positive contribution to MC, based on the finding that mobilities (see Fig. 3), as seen under in-plane B fields, are only limited by scattering at the interfaces. In other words, there is a significant probability for electrons being scattered at one interface with a certain spin direction to reach the other interface without being scattered in between. For the resistance, Umklapp scattering processes ($k_\parallel \rightarrow -k_\parallel$) are most efficient, but are forbidden on the same surface for simple Coulomb scattering due to spin-momentum locking in Rashba-split surface states [51,52], i.e., also Umklapp of the spin is required. Due to the Rashba effect, however, the spin-split states at the other interface have the *opposite* spin direction at the same $k_\parallel$, whereas those at $-k_\parallel$ have the *same* spin direction due to the opposite sign of the potential gradient. Therefore, $k_\parallel \rightarrow -k_\parallel$ scattering processes involving both surfaces *without* spin Umklapp are allowed, as shown in the sketch of Fig. 9.

By turning on a magnetic field, detuning of the sketched process occurs, but only, if the Rashba-splitting at both interfaces is not identical. In fact, due to the screening by the substrate, the interface to Si should exhibit a smaller Rashba splitting than the vacuum interface. With $B \neq 0$ the Zeeman contribution leads to a mismatch of the two Fermi surfaces $\propto B$, resulting in a corresponding phase mismatch between electrons scattered from $+k_\parallel$ at one interface to $-k_\parallel$ at the other. Thus the projections of equivalent wave functions at the two interfaces onto each other get smaller, i.e., the backscattering probability gets smaller in presence of a magnetic field $\propto B^2$ for small dephasing angles. Thus ΔG must be positive as a function of B, as observed. Although this process should exist for B fields in all in-plane directions, only B-field components perpendicular to the current, i.e. those affecting electron motion in current direction, can have an effect on resistance due to the ballistic nature of the scattering process, in agreement with our finding.

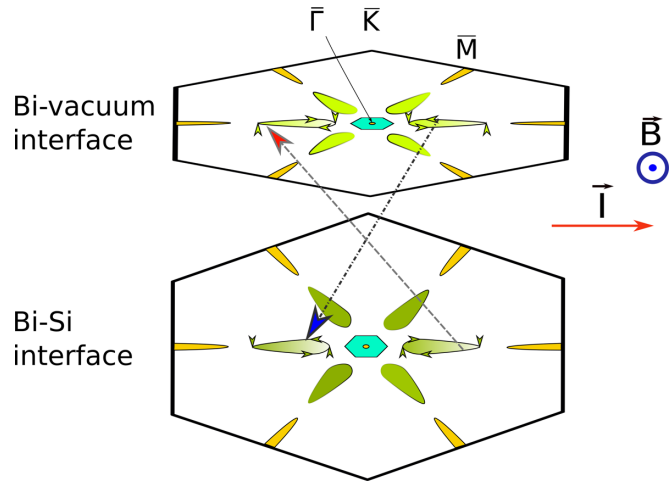

FIG. 9. Illustration of efficient backscattering between Rashba-split interface states (perspective view). For that purpose the Fermi surfaces of both interfaces within the first Brillouin zone are drawn with contours of Rashba split surface states (green, only outer contours with preferential spin direction). Two exemplary backscattering processes $k_\parallel \rightarrow -k_\parallel$ are indicated by dashed lines that do not require spin Umklapp. Relevant are only scattering events along the current direction I. The in-plane magnetic field distorts the $(k_\parallel, -k_\parallel)$ symmetry.

The linear increase of amplitude C, observed for $d \geqslant 50$ BL, is easy to be explained, since it turns out to be directly coupled to the overall linear increase of conductance as a function of d in this range of d (see Fig. 3). This increase is mainly due to the increase of mobilities after full development of the conducting channel through the quantum well state(s). Since all these scattering processes are linear in d, this result means that there is a constant fraction of scattering events at the interfaces that happen by this quasicoherent mechanism.

Summarizing this peculiar scenario, by increasing the thickness of the Bi layers, electronic transport through the whole volume of the quantum film is switched on by partial occupation of a quantized bulk state close to the $\overline{M}$ point. There are three signatures in magnetotransport introduced by this quantum well state: Diffuse scattering, weak localization, and modified weak antilocalization. These processes are all 2D isotropic. However, since the mobilities in these quantum films turn out to be limited only by interface scattering, there is a probability for spin dependent ballistic scattering between the (unequally) spin split interface states that leads to a positive and anisotropic contribution to magnetoconductance. For this effect the quantum well state only plays the role of an efficient transmitter that does not exist without occupation of

this state. Although this situation seems to be similar to topological insulator films with overlapping bulk states [53,54], such phenomena have not been seen there.

IV. SUMMARY AND CONCLUSIONS

Our present results have revealed an intriguing relationship between the transport properties and the electronic states of Bi films. Systematic investigations of magnetoconductance of films with a thickness of 20 BL to 100 BL were conducted at 9 K in parallel magnetic fields up to 4 T. The study of this system in magnetic fields oriented parallel to the surface plane indeed resulted in new insights into the transport properties of these quantum films:

(a) For the thinnest films mainly the surface states are responsible for MC leading to a clear signature of WAL of two coupled interface states with decreasing coupling as a function of thickness.

(b) Although this coupling is evident, there is still no measurable contribution in MC to diffuse scattering from these states in parallel fields, contrary to the field orientation normal to the surface plane, i.e., diffuse scattering between the interface states is very small.

(c) The hybridization of surface states with quantum well states in ultrathin quantum films lifts partially the strict separation between bulk and surface states, as we stated already previously [23]. This has consequences not only for the diffuse scattering in magnetoconductance, once a quantum well state gets partially occupied with increasing film thickness, but also the quantum corrections to MC are modified: By changes of the ratios between scattering lengths, a component of WL is introduced, while the WAL signature is changed. No indications for the appearance of more than one conduction channel were found.

(d) This hybridization also leads to the appearance of an anisotropic and positive correction to MC that was identified as being due to ballistic spin dependent scattering between the interfaces. Thus it is an interference effect between Rashba split surface bands at the interfaces. The possibility to tune this effect either by modifications of the interface properties of by electric fields, similar to experiments in ring structures of semiconducting quantum wells [55,56], has not been exploited yet.

(e) The explicit involvement of surface properties suggests a strong sensitivity to details of the interface structure and to capping layers and may explain the only partial agreement with results published previously [32,33].

ACKNOWLEDGMENT

This work has been supported by the Deutsche Forschungsgemeinschaft through Projects No. Pf238/31 and No. Te386/17-1.

[1] K. Behnia, L. Balicas, and Y. Kopelevich, Science **317**, 1729 (2007).
[2] L. Li, J. G. Checkelsky, Y. S. Hor, C. Uher, A. F. Hebard, R. J. Cava, and N. P. Ong, Science **321**, 547 (2008).
[3] T. Hirahara, T. Nagao, I. Matsuda, G. Bihlmayer, E. V. Chulkov, Y. M. Koroteev, P. M. Echenique, M. Saito, and S. Hasegawa, Phys. Rev. Lett. **97**, 146803 (2006).
[4] H. T. Chu, X.-D. Qi, and F. Yao, Phys. Rev. B **38**, 3653 (1988).
[5] Y. Park, Y. Hirose, S. Nakao, T. Fukumura, J. Xu, and T. Hasegawa, Appl. Phys. Lett. **104**, 023106 (2014).
[6] D. Hsieh, D. Qian, L. Wray, Y. Xia, Y. S. Hor, R. J. Cava, and M. Z. Hasan, Nature (London) **452**, 970 (2008).
[7] T. Sato, K. Yamada, T. Kosaka, S. Souma, K. Yamauchi, K. Sugawara, T. Oguchi, and T. Takahashi, Phys. Rev. B **102**, 085112 (2020).
[8] N. Wang, L. Zhang, T. Wang, H. Yang, Y. Dai, and Y. Qi, J. Appl. Phys. **127**, 025105 (2020).
[9] Chandan, S. Islam, V. Venkataraman, A. Ghosh, and B. Angadi, J. Phys. D **53**, 425102 (2020).
[10] Y. A. Soh and G. Aeppli, Nature (London) **417**, 392 (2002).
[11] A. Husmann, J. B. Betts, G. S. Boebinger, A. Migliori, T. F. Rosenbaum, and M. L. Saboungi, Nature (London) **417**, 421 (2002).
[12] S. Ito, B. Feng, M. Arita, A. Takayama, R.-Y. Liu, T. Someya, W.-C. Chen, T. Iimori, H. Namatame, M. Taniguchi, C.-M. Cheng, S.-J. Tang, F. Komori, K. Kobayashi, T.-C. Chiang, and I. Matsuda, Phys. Rev. Lett. **117**, 236402 (2016).
[13] A. Takayama, T. Sato, S. Souma, T. Oguchi, and T. Takahashi, Nano Lett. **12**, 1776 (2012).
[14] C. R. Ast and H. Höchst, Phys. Rev. Lett. **87**, 177602 (2001).
[15] S. Ito, M. Arita, J. Haruyama, B. Feng, W.-C. Chen, H. Namatame, M. Taniguchi, C.-M. Cheng, G. Bian, S.-J. Tang, T.-C. Chiang, O. Sugino, F. Komori, and I. Matsuda, Sci. Adv. **6**, eaaz5015 (2020).
[16] Y. M. Koroteev, G. Bihlmayer, J. E. Gayone, E. V. Chulkov, S. Blügel, P. M. Echenique, and P. Hofmann, Phys. Rev. Lett. **93**, 046403 (2004).
[17] T.-R. Chang, Q. Lu, X. Wang, H. Lin, T. Miller, T.-C. Chiang, and G. Bian, Crystals **9**, 510 (2019).
[18] T. Hirahara, J. Electron Spectrosc. Relat. Phenom. **201**, 98 (2015).
[19] M. Aitani, T. Hirahara, S. Ichinokura, M. Hanaduka, D. Shin, and S. Hasegawa, Phys. Rev. Lett. **113**, 206802 (2014).
[20] Z. Hou, C. Gong, Y. Wang, Q. Zhang, B. Yang, H. Zhang, E. Liu, Z. Liu, Z. Zeng, G. Wu, W. Wang, and X.-X. Zhang, J. Phys.: Condens. Matter **30**, 085703 (2018).
[21] N. Miyata, K. Horikoshi, T. Hirahara, S. Hasegawa, C. M. Wei, and I. Matsuda, Phys. Rev. B **78**, 245405 (2008).
[22] M. Henzler, T. Lüer, and J. Heitmann, Phys. Rev. B **59**, 2383 (1999).
[23] D. Abdelbarey, J. Koch, Z. Mamiyev, C. Tegenkamp, and H. Pfnür, Phys. Rev. B **102**, 115409 (2020).
[24] N. Marcano, S. Sangiao, C. Magén, L. Morellón, M. R. Ibarra, M. Plaza, L. Pérez, and J. M. De Teresa, Phys. Rev. B **82**, 125326 (2010).
[25] C. J. Lin, X. Y. He, J. Liao, X. X. Wang, V. S. IV, W. M. Yang, T. Guan, Q. M. Zhang, L. Gu, G. Y. Zhang, C. G. Zeng, X. Dai, K. H. Wu, and Y. Q. Li, Phys. Rev. B **88**, 041307(R) (2013).

[26] H. B. Zhang, H. L. Yu, D. H. Bao, S. W. Li, C. X. Wang, and G. W. Yang, Phys. Rev. B **86**, 075102 (2012).
[27] H. Wang, H. Liu, C.-Z. Chang, H. Zuo, Y. Zhao, Y. Sun, Z. Xia, K. He, X. Ma, X. C. Xie, Q.-K. Xue, and J. Wang, Sci. Rep. **4**, 5817 (2014).
[28] D. Lükermann, S. Sologub, H. Pfnür, and C. Tegenkamp, Phys. Rev. B **83**, 245425 (2011).
[29] N. Miyata, R. Hobara, H. Narita, T. Hirahara, S. Hasegawa, and I. Matsuda, Jpn. J. Appl. Phys. **50**, 036602 (2011).
[30] T. Hirahara, I. Matsuda, S. Yamazaki, N. Miyata, S. Hasegawa, and T. Nagao, Appl. Phys. Lett. **91**, 202106 (2007).
[31] P. Kröger, D. Abdelbarey, M. Siemens, D. Lükermann, S. Sologub, H. Pfnür, and C. Tegenkamp, Phys. Rev. B **97**, 045403 (2018).
[32] F. Pang, Chin. Phys. Lett. **32**, 027402 (2015).
[33] S.-L. Yin, X.-J. Liang, and H.-W. Zhao, Chin. Phys. Lett. **30**, 087305 (2013).
[34] D. Lükermann, S. Sologub, H. Pfnür, C. Klein, M. Horn-von Hoegen, and C. Tegenkamp, Phys. Rev. B **86**, 195432 (2012).
[35] B. L. Al'tshuler and A. G. Aronov, JETP Lett. **33**, 499 (1981).
[36] S. Maekawa and H. Fukuyama, J. Phys. Soc. Jpn. **50**, 2516 (1981).
[37] C. W. J. Beenakker and H. van Houten, Phys. Rev. B **38**, 3232 (1988).
[38] O. E. Raichev and P. Vasilopoulos, J. Phys.: Condens. Matter **12**, 589 (2000).
[39] A. B. Pippard, *Magnetoresistance in Metals* (Cambridge University Press, Cambridge 1989).
[40] S. Das, Z. Hossain, and R. C. Budhani, Phys. Rev. B **94**, 115165 (2016).
[41] V. K. Dugaev and D. E. Khmel'nitskii, Sov. Phys. JETP **59**, 1038 (1984).
[42] E. Kneedler, D. Skelton, K. E. Smith, and S. D. Kevan, Phys. Rev. Lett. **64**, 3151 (1990).
[43] Z. Zhu, A. Collaudin, B. Fauqué, W. Kang, and K. Behnia, Nat. Phys. **8**, 89 (2012).
[44] L. N. Oveshnikov, V. A. Prudkoglyad, Y. G. Selivanov, E. G. Chizhevskii, and B. A. Aronzon, JETP Lett. **106**, 526 (2017).
[45] Y. A. Bychkov and E. I. Rashba, J. Phys. C **17**, 6039 (1984).
[46] G. Dresselhaus, Phys. Rev. **100**, 580 (1955).
[47] A. G. Mal'shukov, K. A. Chao, and M. Willander, Phys. Rev. B **56**, 6436 (1997).
[48] A. G. Mal'shukov, V. A. Froltsov, and K. A. Chao, Phys. Rev. B **59**, 5702 (1999).
[49] J. Schliemann and D. Loss, Phys. Rev. B **68**, 165311 (2003).
[50] G. Cantele and D. Ninno, Phys. Rev. Mater. **1**, 014002 (2017).
[51] F. Vas'ko, JETP Lett. **30**, 541 (1979).
[52] M. Kohda, T. Okayasu, and J. Nitta, Sci. Rep. **9**, 1909 (2019).
[53] R. K. Gopal, S. Singh, A. Mandal, J. Sarkar, and C. Mitra, Sci. Rep. **7**, 4924 (2017).
[54] Z. Ren, A. A. Taskin, S. Sasaki, K. Segawa, and Y. Ando, Phys. Rev. B **82**, 241306(R) (2010).
[55] F. Nagasawa, A. A. Reynoso, J. B. Baltanás, D. Frustaglia, H. Saarikoski, and J. Nitta, Phys. Rev. B **98**, 245301 (2018).
[56] H. Saarikoski, A. A. Reynoso, J. P. Baltanás, D. Frustaglia, and J. Nitta, Phys. Rev. B **97**, 125423 (2018).